

*Subarea characteristics of the long-range correlations and the index  $\chi$  for daily temperature records over China*

**Lei Jiang, Naiming Yuan, Zuntao Fu,  
Dongxiao Wang, Xia Zhao & Xiuhua  
Zhu**

**Theoretical and Applied Climatology**

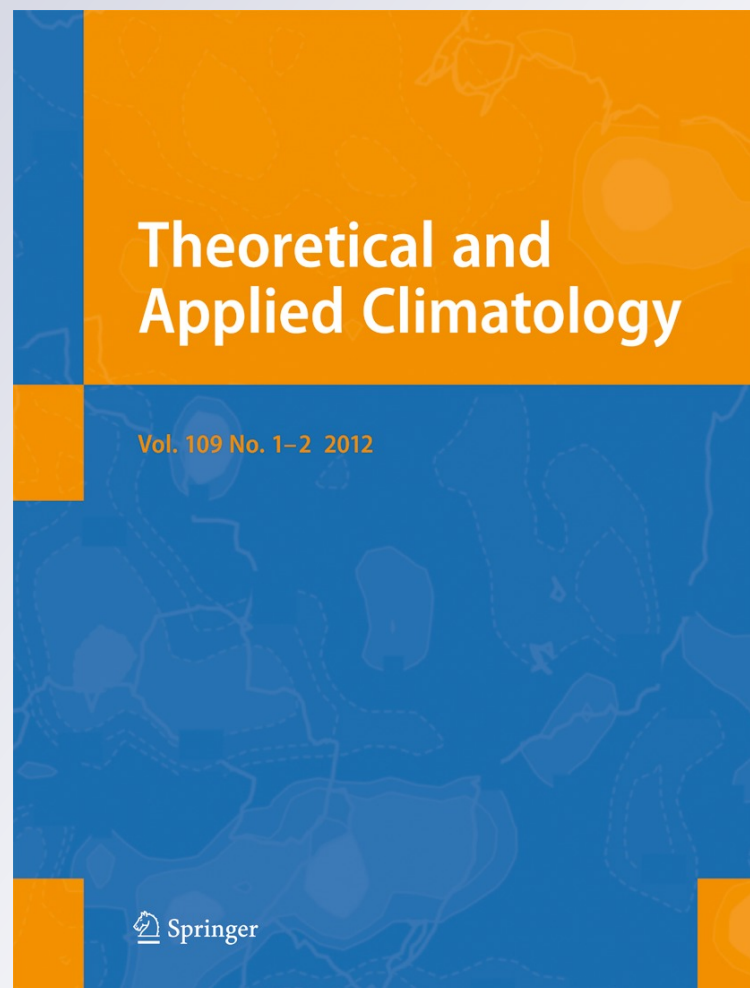
ISSN 0177-798X

Volume 109

Combined 1-2

Theor Appl Climatol (2012) 109:261-270

DOI 10.1007/s00704-011-0578-6



**Your article is protected by copyright and all rights are held exclusively by Springer-Verlag. This e-offprint is for personal use only and shall not be self-archived in electronic repositories. If you wish to self-archive your work, please use the accepted author's version for posting to your own website or your institution's repository. You may further deposit the accepted author's version on a funder's repository at a funder's request, provided it is not made publicly available until 12 months after publication.**

# Subarea characteristics of the long-range correlations and the index $\chi$ for daily temperature records over China

Lei Jiang · Naiming Yuan · Zuntao Fu ·  
Dongxiao Wang · Xia Zhao · Xiuhua Zhu

Received: 21 October 2010 / Accepted: 21 December 2011 / Published online: 10 January 2012  
© Springer-Verlag 2012

**Abstract** Daily temperature records including daily minimum, maximum, and average temperature from 190 meteorological stations over China during 1951–2000 are analyzed from two perspectives: (a) long-term persistence in direction of time varies, and (b) standard deviation in direction of amplitude varies. By employing the detrended fluctuation analysis (DFA), we find all the temperature records are long-term correlated, while the exponent  $\alpha$  obtained from DFA varies from different districts of China due to different climate conditions, such as the southwest

monsoon, subtropical high, northeast cold vortex, and the Tibetan plateau, etc. After we take the standard deviation into account, a new index  $\chi = \alpha \times \sigma$ , which has been proposed recently, can be obtained. By further rescaling it as  $\chi = \bar{\chi} - 1/5 \times \sigma_{\bar{\chi}}$ , we find an obvious change of  $\chi$  for these three kinds of time series, from which the whole China can be divided into two groups, which are comparatively consistent with dry/wet distributions in the south–north areas over China.

L. Jiang · N. Yuan · Z. Fu  
Department of Atmospheric and Oceanic Sciences and Laboratory  
for Climate and Ocean- Atmosphere Studies, School of Physics,  
Peking University,  
Beijing, China

L. Jiang · D. Wang  
LED, South China Sea Institute of Oceanology,  
Chinese Academy of Sciences,  
Guangzhou, China

X. Zhao  
Laboratory of Ocean Circulation and Waves,  
Institute of Oceanology, Chinese Academy of Sciences,  
Qingdao, China

L. Jiang  
State Key Laboratory of Remote Sensing Science,  
Institute of Remote Sensing Application,  
Chinese Academy of Sciences,  
Beijing, China

X. Zhu  
Max Planck Institute for Meteorology,  
Hamburg, Germany

Z. Fu (✉)  
School of Physics, Peking University,  
Beijing 100871, China  
e-mail: fuzt@pku.edu.cn

## 1 Introduction

The current global temperature changes are the issues concerned extensively by the scientific communities, society, and the public. Jones (1988) calculated the changes of the annual average temperature trends from 1967 to 1986 in the northern hemisphere and found the greatest warming districts mainly in Russia (especially Western Siberia), Alaska, the northwest of Canada and the southwest of Europe et al. The Intergovernmental Panels on Climate Change (IPCC) in 1990 scientific assessment reports also pointed out: the global temperature increases 0.5°C/10a of linear warming trend rates from 1980 to 1989 (WMO and UNEP 1990). Robert et al., (2001) pointed out that the average global surface temperature since 1861 has increased  $0.6 \pm 0.2^\circ\text{C}$  during the twentieth century in The Third Assessment Report on Climate Changes. The global temperature had warming trends on the second half of the last century (Dai et al. 1998; Zhai and Pan 2003; Zhai et al. 2004; Zou et al. 2005). At the same time, the temperature has increased by 1°C to 2°C in the northwest regions of North America (Hansen et al. 1998; Cayan et al. 2001). All projections of future change indicate that the warming is likely to continue, and this conclusion holds regardless of the computer model

used or the emission scenario applied in the model (Zwiers 2002). A recent test (Govindan et al. 2002) demonstrated that the scaling performance of seven leading global climate models by using detrended fluctuation analysis failed to reproduce the universal scaling behavior of six observed temperature records by underestimating the long-range persistence of the atmosphere and overestimating the trends, suggests that the anticipated global warming is also overestimated by the models. Moreover, other tests, such as (Vyushin et al. 2004; Rybski et al. 2008) on the performance of more advanced climate models where volcanic activity has been taken into, had much better results. On the other hand, Fraedrich and Blender (2003) demonstrated that coupled atmosphere–ocean models are able to reproduce the observed behavior up to decades and long-time memory on centennial time scales is found only with a comprehensive ocean model. In any case, direct comparison of local observations with the rather low resolution general circulation models might have many pitfalls (Pielke et al. 2002). Therefore an extended analysis of measured asymptotic correlations is a prerequisite. The facts show that the climate changes are vastly different over different areas. Therefore, the temperature fluctuation need be discussed and studied for regional change. The average temperature reflects on the average extents of a regional temperature change, which was generally considered to be unbiased and fulfilled the normal distributions. The highest and lowest temperature has important effect on the extreme events of climate and weather systems. Therefore, the research to the highest and lowest temperature is very necessary and meaningful.

## 2 Data records and method

The data sets taking part in international exchange processed by Chinese National Meteorological Information Center have been applied in present work, which are high-quality daily land surface climatic records including 194 Chinese meteorological stations. The same records were utilized in many studies to analyze climate change over China in the recent 50 years (Zhai et al. 2004; Zou et al. 2005). Data for three stations, station 54618, 52203, and 54909, were kicked out for their short time range about 10 years, while records of the other stations last about 50 years, from 1951 to 2000. According to Chen et al. (2002), scaling of correlated data series are not affected by randomly cutting out segments and stitching together the remaining parts, even when 50% of the points are removed. Therefore, we remove the missing values from the raw data over some stations, since they are only a little part of series. The main data sets used in this work are daily temperature time series which includes daily mean, minimum, maximum temperature. On

one hand, to overcome the natural non-stationarity of the temperature data due to season trends, we remove the annual cycle from the raw data  $T_i$  (daily temperatures) by computing the anomaly series  $\Delta T_i = T_i - \langle T_i \rangle_d$  for temperatures, where  $\langle \rangle_d$  denotes the long-time average value for the given calendar day. On the other hand, to overcome the crossover effect by calculating fluctuation function changing with the bin  $s$  in the double logarithmic coordinates, we pick out the straight section which has removed the small-scale parts to get the accurate scaling exponent, which can be meaningful to consider the time series persistence.

The basic method—detrended fluctuation analysis (DFA)—which was introduced by Peng et al. (1994), and extended by Bunde et al. (2000) and Kantelhardt et al. (2001), has been successfully applied to a variety of systems ranging from DNA (Peng et al. 1994, 1995), atmospheric temperature (Bunde et al. 1998; Govindan et al. 2003; Kurnaz 2004a; Kiraly and Janosi 2005), and SST (Bunde and Havlin 2002; Monetti et al., 2003). Following the work of Peng et al. (1994, 1995), several theoretical studies elucidated the power and limitations of filtering out various trends from synthetic data series (Heneghan and McDarby 2000; Talkner and Weber 2000; Hu et al. 2001).

The DFA procedure consists in the following steps (Kantelhardt et al. 2001):

1. Daily temperature data have a non-stationary nature due to seasonal trends. As a first step of DFA analysis, the annual cycle is removed from the raw data  $T_i$  by computing the temperature anomaly series  $\Delta T_i = T_i - \langle T_i \rangle_d$ ,  $i = 1, \dots, N$ ,  $\langle \rangle_d$  denotes the long-time average for the given calendar day.
2. An integrated time series (also called “profile”)  $Y(m)$ ,  $m = 1, \dots, N$ , is then obtained as follows:

$$Y(m) = \sum_{i=1}^m \Delta T_i, \quad (m = 1, 2, \dots, N)$$

In the second step, we cut the profile  $Y(m)$  into  $N_s \equiv [N/s]$  non-overlapping segments of equal length  $s$ . Since the record length  $N$  need not be a multiple of the considered time scale  $s$ , a short part at the end of the profile will remain in most cases. In order not to disregard this part of the record, the same procedure is repeated starting from the other end of the record. Thus,  $2N_s$  segments are obtained altogether (Bunde et al. 1996; Govindan et al. 2001; Kantelhardt et al. 2001; Bunde et al. 2006).

3. In the third step, we calculate the local trend for each segment  $s$  by a least squares fit of the data. Then we define the  $y$  coordinate of the fitting line in each box is indicated by  $Y_s(m)$ . The integrated signal  $Y(m)$  is

detrended by subtracting the local trend  $P_s(m)$  in each box of length  $s$ , as the difference between the original time series and the fits:

$$Y_s(m) = Y(m) - P_s(m)$$

Linear, cubic, or higher order polynomials can also be used in the fitting procedure (DFA1, DFA3, and higher order DFA). Since the detrending of the time series is done by the subtraction of the fits from the profile, these methods differ in their capability of eliminating trends in the data. In  $n$ th order DFA, trends of order  $n$  in the profile and of order  $n-1$  in the original record are eliminated. Thus, a comparison of the results for different orders of DFA allows to estimate the strength of the trends in the time series.

- For given  $s$ -size box, the root-mean-square fluctuation function,  $F(s)$ , for this integrated and detrended signal is given by

$$F(s) = \left[ \frac{1}{2N_s} \sum_{k=1}^{2N_s} (Y(k) - Y_s(k))^2 \right]^{\frac{1}{2}}$$

- The scaling behavior of the fluctuation functions is determined by analyzing the log-log plots  $F(s)$  versus  $s$ . If the original series  $\{T_i\}$  is long-range power-law correlated, the fluctuation function will vary as

$$F(s) \propto s^\alpha$$

It is apparent that the variance will increase linearly with increasing duration  $s$  of the segments in the double logarithmic coordinates within a certain scaling range. The slope value  $\alpha$  represents the degree of the correlation in the signal: if  $\alpha=0.5$ , the signal is uncorrelated (white noise); if  $\alpha>0.5$ , the signal is correlated; if  $\alpha<0.5$ , the signal is anticorrelated, for  $\alpha=1$ , the signal is  $1/f$  noise. Different orders  $n$  of DFA (DFA1, DFA2, etc.) differ in the order of the polynomials used in the fitting procedure.

### 3 The LRC and its regional characteristics for daily min, max, average temperature records

Firstly, we choose two examples for Stations Beijing and Xiamen randomly to calculate the profiles and the slopes by the DFA2. It is apparent that the profiles show different shapes in Fig. 1a. The temperature profile for station Beijing

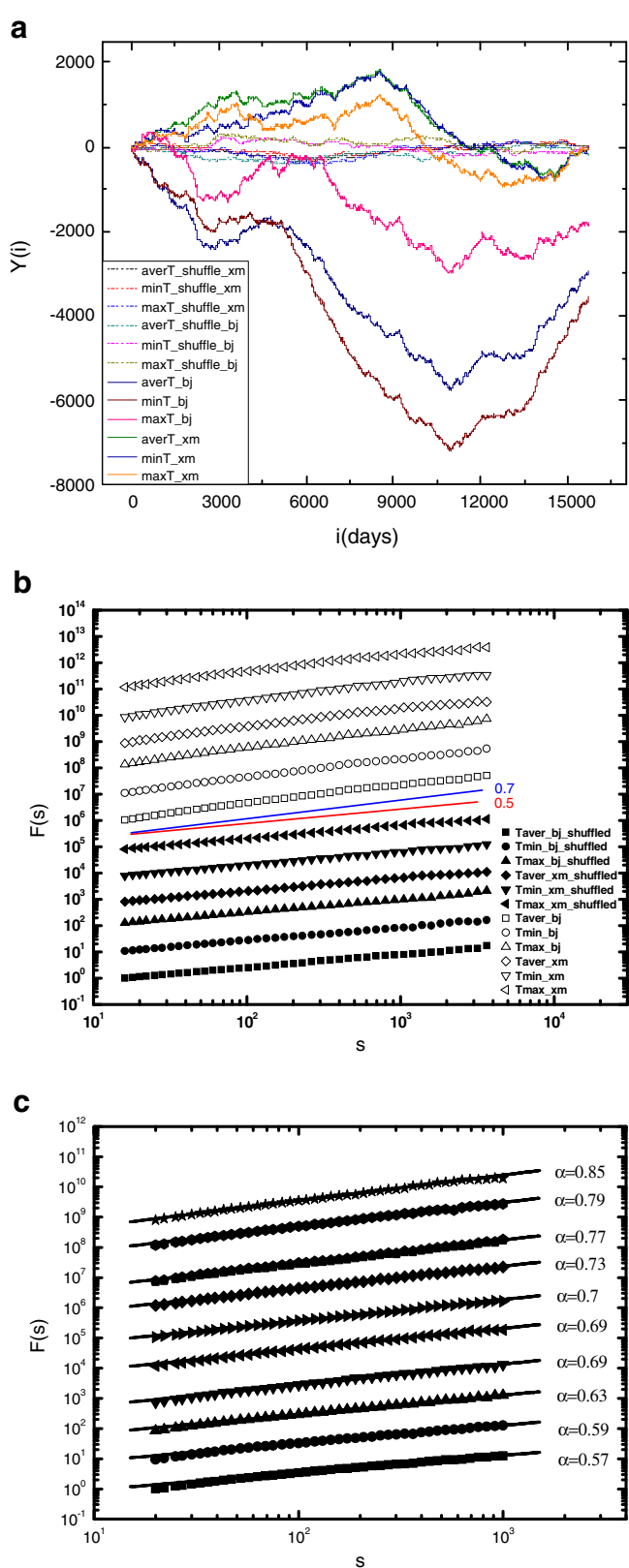
decreases below the value 0 till the time scale is about 11,000 days and then increases, taking on a shape just like the letter “v”. While the profile for station Xiamen firstly increases above the value 0 and then decreases till the value of the profile is smaller than -800, which may indicate the presence of a negative linear trend, taking on a shape just like the letter “^”. The profiles exhibit similar behaviors for the min, max, average temperature records. The trends of the max temperature series for two stations are weaker than those of the min, average temperature records, especially for the min temperature in Beijing, the profile fluctuation is the largest, which implies positive linear trends. Secondly, in order to further detect the LRC, we have plotted fluctuation function  $F(s)$  for Stations Beijing and Xiamen, see Fig. 1b. The existence of crossovers in DFA curves, which may be due to general weather situation (or Grosswetterlagen), but not due to a broad probability distribution (Bunde et al. 1998, 2006; Bunde et al. 2004). So, it is imperative that we remove the trends and correlations by randomly shuffling the daily temperature data sets for station Beijing and Xiamen in order to test the LRC. Figure 1a (dash lines) and b (solid lines) show the profiles and fluctuation results by the DFA2 for the shuffled data for the above two stations, respectively. It is obvious that the DFA-exponents over stations Beijing and Xiamen are about 0.5 just as expected.

Figure 1b shows that the temperature records exhibit the same slopes in each case, this similar behavior has been observed before for daily temperature data (Talkner and Weber 2000; Weber and Talkner 2001; Kurnaz 2004b). In addition, due to the lack of statistical significance for large scale, the curves above 3 years should not be taken into account (Hu et al. 2001). In the present work, we apply the results of our analysis for daily temperature data at all the weather stations for long time scales between  $s>30$  days and  $s<3$  years to study temperature fluctuations for 190 weather stations over China. The DFA-exponents are  $\alpha_{\min}=0.70, 0.70; \alpha_{\max}=0.70, 0.67; \alpha_{\text{aver}}=0.71, 0.68$ , corresponding to the min, max, average temperature in station Beijing and Xiamen, respectively. By calculations, the temperature fluctuations are found to be power-law correlated. Positive long-range correlations are detected from 30 days to 3 years for each station, in which the range of this power law seems to exceed one decade for the temperature records, and their scaling exponents vary from station to station. See Fig. 1c, results of ten representative average temperature records from different districts are shown. From bottom to top, the Hurst exponent  $\alpha$  is 0.57 (Wuqiaoling), 0.59 (Wuzhou), 0.63 (Nanjing), 0.69 (Ganzi), 0.69 (Daerhanlianheqi), 0.7 (Shenyang), 0.73 (Huma), 0.77 (Qumalai), 0.79 (Kelamayi), 0.85 (Tulufan). We can see that even for the outliers ( $\alpha=0.77, 0.79, 0.85$ ), there are still good scaling behaviors within the above ranges. We would like to note that, according to Rybski and Bunde (2009) and Lennartz and Bunde

**Fig. 1** **a** The profiles of the min, max, aver temperature (solid lines) and shuffled records (dash lines) for station Beijing and Xiamen during the time from 1951 to 2000. **b** The double log-log plot of the power law relationship between the detrended variability  $F(s)$  and the time scale  $s$  over station Beijing and Xiamen. Blue line is the curve of linear fit for the real data. Red line is the curves of linear fit for the shuffled data. From bottom to top, are the results of the max, the min, the aver for Xiamen, and the max, the min, the aver for Beijing. Full symbols represent the results from shuffled records and open symbols for the real records **c** DFA2 for ten representative average temperature records from different districts. From bottom to top, the Hurst exponent  $\alpha$  is 0.57 (Wuqiaoling), 0.59 (Wuzhou), 0.63 (Nanjing), 0.69 (Ganzi), 0.69 (Daerhanlianheqi), 0.7 (Shenyang), 0.73 (Huma), 0.77 (Qumalai), 0.79 (Kelamayi), 0.85 (Tulufan). The DFA curves have been shifted by factor of 10

(2009), DFA-exponents can scatter tremendously if we obtain the sub-record (e.g., with length of 2,000) from a long (e.g., with length of 2 million) record characterized by a DFA-exponents  $\alpha$ . However, if the length of the sub-record increases to 20,000 (which is similar to the length of the records analyzed in our work), the standard deviation of the DFA-exponents  $\alpha$  is only around 0.01, which is smaller compared with the standard deviations (around 0.05) obtained in our work. Thus, the non-universality of the scaling behaviors cannot be excluded.

Figure 2 gives frequency distributions of the scaling exponents obtained from these 190 stations. As we can see, consistent with the earlier observations (Bunde et al. 1996, 1998; Govindan et al. 2002; Eichner et al. 2003), long-term correlations exist, with the range of the scaling exponents from 0.57 to 0.90. For these 190 weather stations, we find that average scaling exponents for the daily aver, min, max temperature records are  $\alpha_{aver}=0.68\pm 0.05$ ;  $\alpha_{min}=0.69\pm 0.05$ ;  $\alpha_{max}=0.66\pm 0.05$ , respectively. The daily temperature fluctuations are found to be power-law correlated for all weather stations over China and many of their scaling exponents, especially in the northeast and northwest districts over China, are higher than that of the temperature fluctuations of earlier claims (Bunde et al. 1996, 1998; Bunde and Havlin 2002). These results indicate that there exists a stronger persistence in daily temperature series fluctuations. Positive long-range correlations are detected from 3 month to 3 years for each case, whose range of this power law seems to exceed one decade in atmospheric temperature (Fraedrich and Blender 2003; Govindan et al. 2003; Monetti et al. 2003). Even though there is some scatter in the data after a period of 10 years, the scatter in the data is still within the error bars of the analysis (Bunde et al. 1998; Bunde et al. 2001; Kiraly and Janosi 2005). Comparing to a universal persistence law  $\alpha=0.65$  for land temperature series of earlier claims (Bunde et al. 1998; Eichner et al. 2003), the daily min, max, average temperature time series over China seems to exhibit a much stronger LRC. In fact, it is obvious that for many stations the daily min, max, average temperature series exhibit stronger persistence for small scale than that



for large scale. A dynamics of increased baroclinicity means that an underlying correlated process can be more often interrupted by short memory, small-scale processes yielding

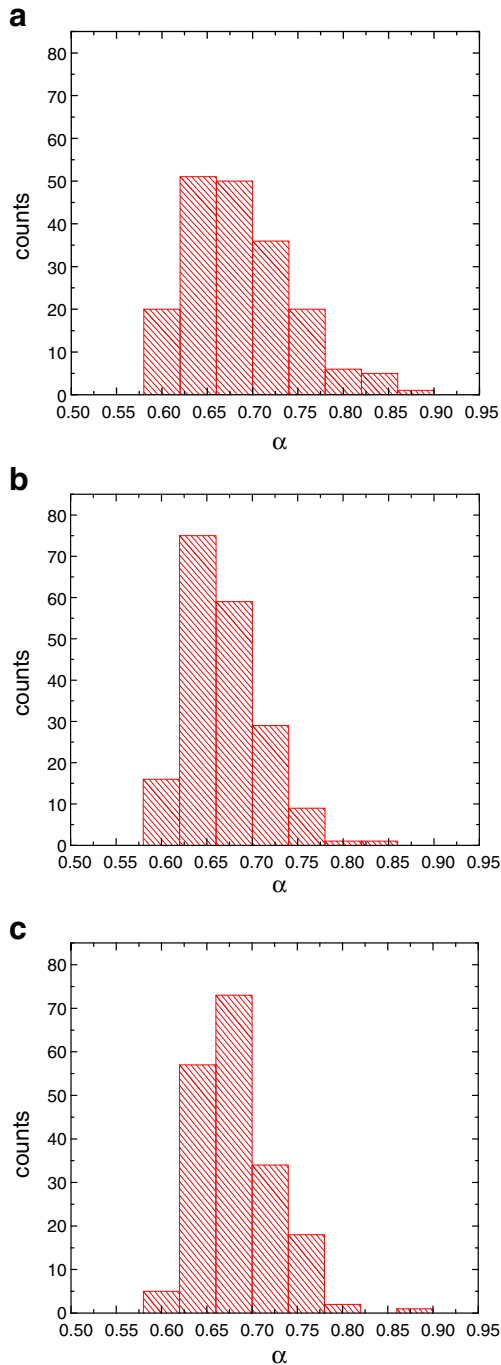


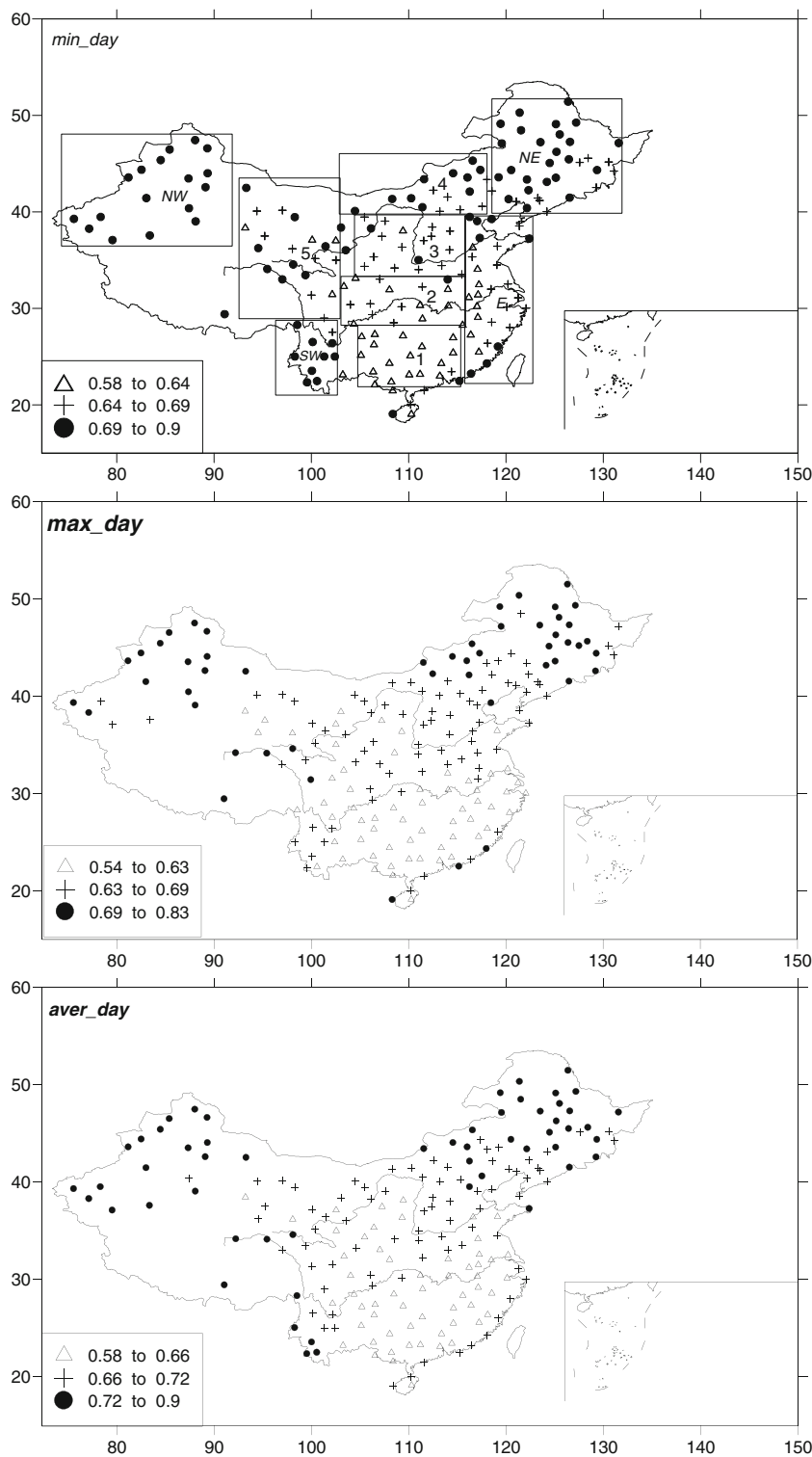
**Fig. 2** The histograms of the scaling exponents for daily min (a), max (b), average temperature series (c). The mean value, skewness, and kurtosis of the slopes from the 190 stations  $\alpha_{\min}=0.69, 0.81, 1.801$ ;  $\alpha_{\max}=0.65, 0.56, -0.19$ ;  $\alpha_{\text{aver}}=0.67, 0.68, 0.99$ , respectively

a decreased effective correlation exponent (Kiraly and Janosi 2005). In addition, for two representative station, skewness=0.81, 0.56, 0.68 and kurtosis=1.801, -0.19, 0.99 respectively demonstrate that the daily temperature fluctuations are non-normal, which imply increasingly trends of temperature.

From area 1 to area 4 in Fig. 3 min\_day, one can see the scaling exponents are gradually increasing with increasing distance from the equator, where the area 3 seems to be a transition belt from south to north, which is not visible on the map given by Fraedrich and Blender (2003) and Kiraly and Janosi (2005), which might be a consequence of their much lower spatial resolution over China. In addition, we may clearly see that the daily temperature fluctuations are found to be power-law correlated and their scaling exponents are not universal for continental stations, which is different from previous results (Bunde et al. 1998; Eichner et al. 2003). Actually, Kiraly and Janosi (2005) have already reported that the correlation exponent is not universal for continental stations over Australia, which is in agreement with our results (see Fig. 3).

Area E in Fig. 3 shows that scaling exponent values are decreasing with the increasing distance from east coastline but within only smaller distances, exponent values turn into latitudinal distributions, which seems not to be affected by sea-land difference. So, we can deem that scaling exponents depend on sea-land difference is weak and sea-land difference affects scaling exponent distributions within only smaller distances from the shore. The results show that the scaling exponents are high in littoral and temperature fluctuations persistence is strong. As can be seen clearly in the southwest region of China, especially Yunnan province, it is obvious that the scaling exponent values in area SW in Fig. 3 are higher than that in the adjacent regions. This may be caused by sea-land difference, southwest monsoon, and big landform etc. factors interactions. The future persistence of temperature shows strong in such area that may be related to the long-term transformation steadily of the southwest monsoon, sea-land difference, and big landform etc. factors interactions. Lastly, there exists a large distribution of the scaling exponent values in area NW and NE in Fig. 3, which may be due to the exchanges of south and north weather systems, Tibet Plateau landform, Siberian high pressure and monsoon and so on. The future temperature change takes on obvious increasing trends. Area 5 seems to be a transition belt that needs analyze further. In conclusion, the daily temperature fluctuations are found to be power-law correlated and their scaling exponents vary from station to station. In other words, the correlation exponents are not universal for continental stations. Numerical simulation results show that, with further intensification of the human activities and incessant increase for the emissions of greenhouse gases, the global climate will be further warming and may lead to more drought in the mid-latitude regions of the northern hemisphere (Manabe et al. 1981; Manabe and Wetherald 1987; Wetherald and Manabe 1999, 2002; Bunde and Havlin 2002). In northern China, the temporal and spatial pattern of precipitation has also undergone a transformation under global temperature warming backgrounds and the persistent droughts appear in some areas (Ma and Fu 2003).

**Fig. 3** The geographical distributions of scaling exponents for daily min, max, average temperature series



Wu and Zhang (1998) and Hsu and Liu (2006) have reported the various climate features of China are major determined by the system of the East Asian and South Asian monsoon. The East Asian summer monsoon system assumes significant variability at intraseasonal, interannual, and even interdecadal time scales, which may have influence on regional characteristics of persistence for daily

temperature records. Therefore, from the fact that the different daily temperature fluctuation scaling exponents are related to different climate system, and that may be caused by East Asian Summer monsoon system, the different temperature fluctuation scaling exponents may reflect the different physical processes and mechanisms monitoring the different climate regions over China.

#### 4 Standard deviation analysis and regional characteristics for the temperature records

The factors that determine the environment conditions in some regions are not only their variation trends, but also variation extents, which are important consulting indicator; therefore, the standard deviation (Std) of the temperature records ( $T_{Std}$ ) is introduced here. To some extent, the Std reflects an extent of the deviating mean value. The Std is larger, the meteorology element fluctuations larger in certain regions, which increase the possibility of extreme weather events. Standard deviation reflects the complicated conditions of the temperature fluctuations and variations in certain extents.

Figure 4 shows  $T_{Std}$  frequency distributions of the temperature records including the daily min, max, average temperature records obtained from these 190 stations over China. the mean value of Std is  $\bar{\sigma}_{min} = 3.40 \pm 0.75^\circ C$ ,  $\bar{\sigma}_{max} = 4.00 \pm 0.65^\circ C$ ,  $\bar{\sigma}_{aver} = 3.20 \pm 0.70^\circ C$ , respectively.  $T_{Std}$  variations of the maximum temperature records are comparatively convergent. There are 61 stations over China, where  $T_{Std}$  frequency distributions are in the range 4.5 to 5.0. In addition, the fluctuations are larger for maximum temperature records than for the other two kinds of records, which imply the increasing possibility of extreme events occurrence.

The skewness describes the non-symmetry distribution characteristics of variable probability density functions. The skewness values are  $\bar{g}_{1(min)} = 0.01 \pm 0.19$ ;  $\bar{g}_{1(max)} = -0.11 \pm 0.27$ ;  $\bar{g}_{1(aver)} = -0.06 \pm 0.24$  for the daily min, max, average temperature records, respectively. This illustrates that it is not apparent for the skewness characteristics of the daily temperature records located around the "0" as a whole. The kurtosis describes the gradients of the distribution curves. The kurtosis values are  $\bar{g}_{2(min)} = 0.50 \pm 0.42$ ;  $\bar{g}_{2(max)} = 0.30 \pm 0.46$ ;  $\bar{g}_{2(aver)} = 0.50 \pm 0.51$ , respectively. There are appreciably increasing trends for Kurtosis more than for normal school.

The Std of the daily max temperature records is larger than that of the min, average temperature series, which may imply the increasing extreme events. The  $T_{Std}$  distributions are similar over China, where there are large fluctuations in the northeast and northwest regions, whereas, small in the Southwest and coastline, as shown in Fig. 5. These results indicate that there are more large probability of abrupt climate changes in the northeast and northwest areas. Inter-decadal changes may cause  $T_{Std}$ 's reduce in the Southwest of China, which further affects the LRC.

#### 5 Subarea characteristics of the index $\chi$ for daily temperature records

In order to synthetically evaluate climate conditions in certain regions, it is imperative that using an index assesses its

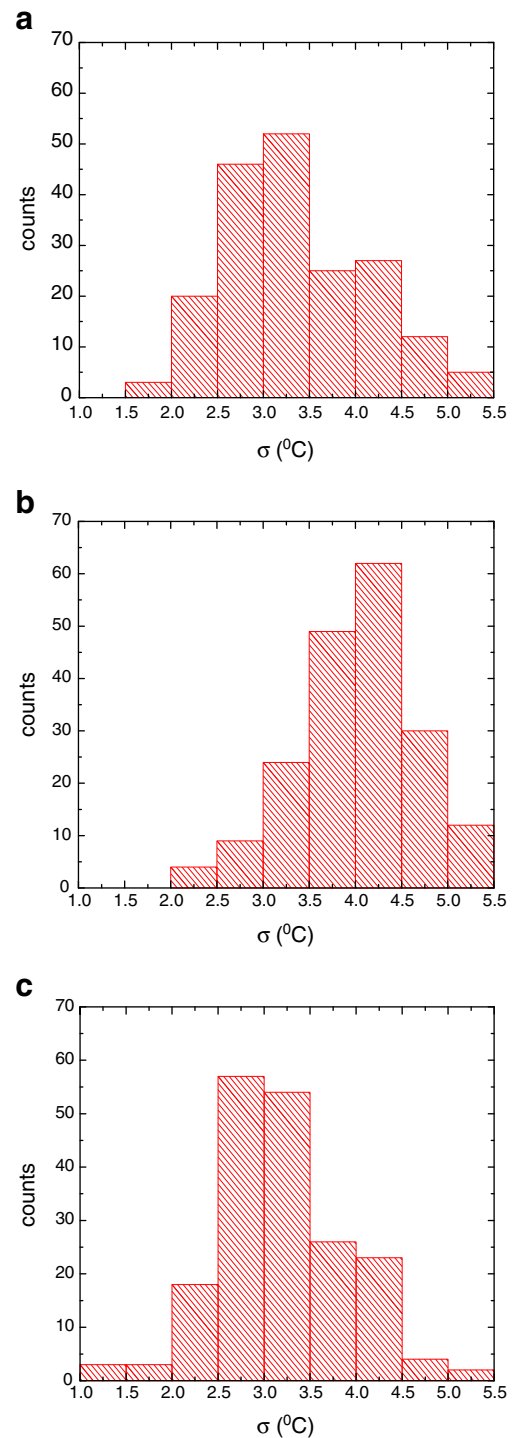
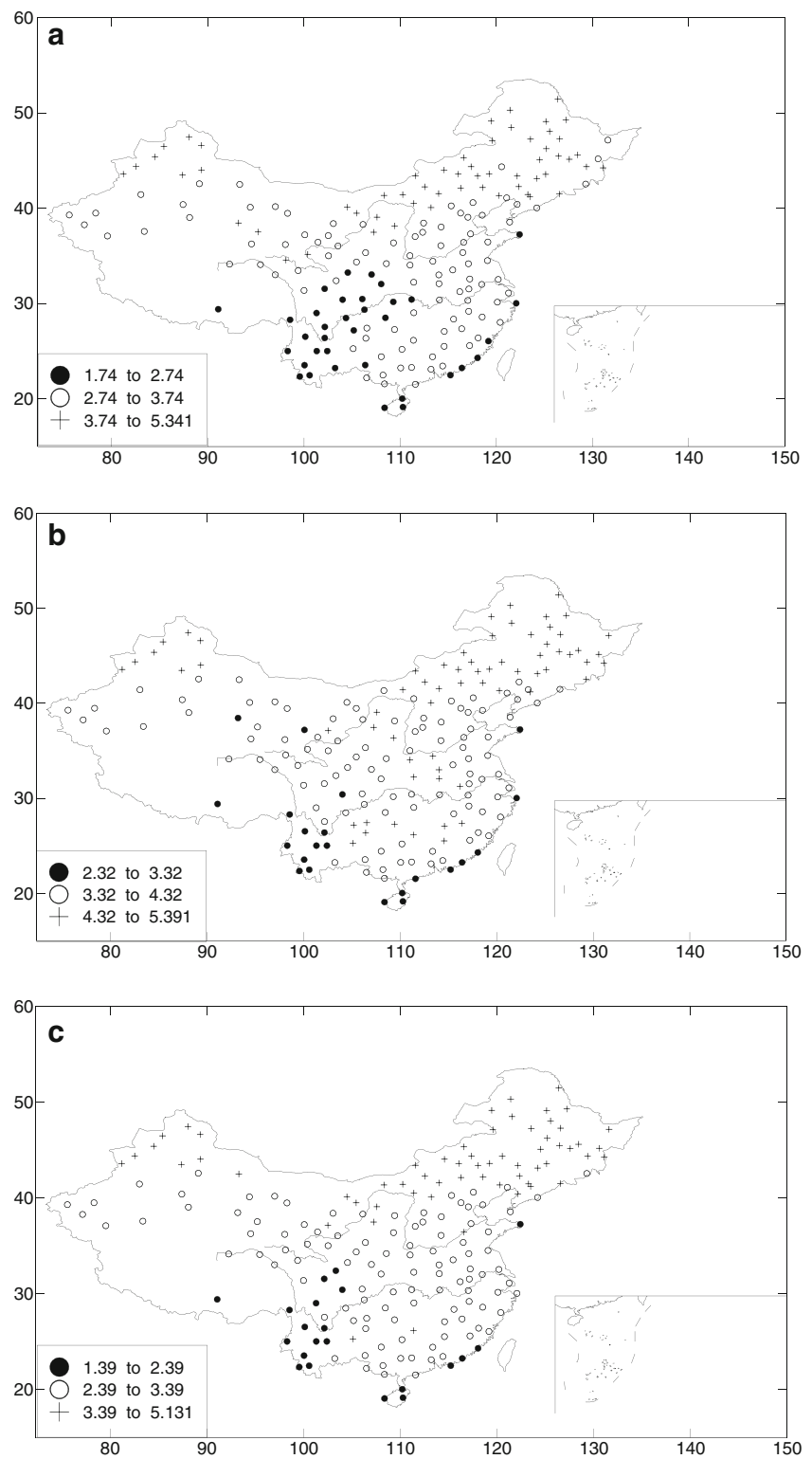


**Fig. 4** Histograms of the temperature Std. **a** Minimum temperature records. **b** Maximum temperature records. **c** Mean temperature records

overall climate change extents. The LRC can reflect variation trends of some climate element fields in the future, which behaves the long-range correlations; whereas, The Std weighs the variation extents of the deviation from mean states in certain areas. We may score better regional distribution characteristics by combination the scaling exponent

**Fig. 5** The geographical distributions of the temperature Std. **a** Minimum temperature records. **b** Maximum temperature records. **c** Mean temperature records



with the Std effectively. Therefore, by using the subarea index  $\chi$  (Chen et al. 2007), its calculation formula:  $\chi = \alpha \times \sigma$  ( $\alpha$ : the scaling exponent of time series,  $\sigma$ : the Std of time series), we gain the significant partition characteristics for the daily temperature records over different regions of China. This may provide some kind of clue on the

extreme events such as high temperature, drought, among others.

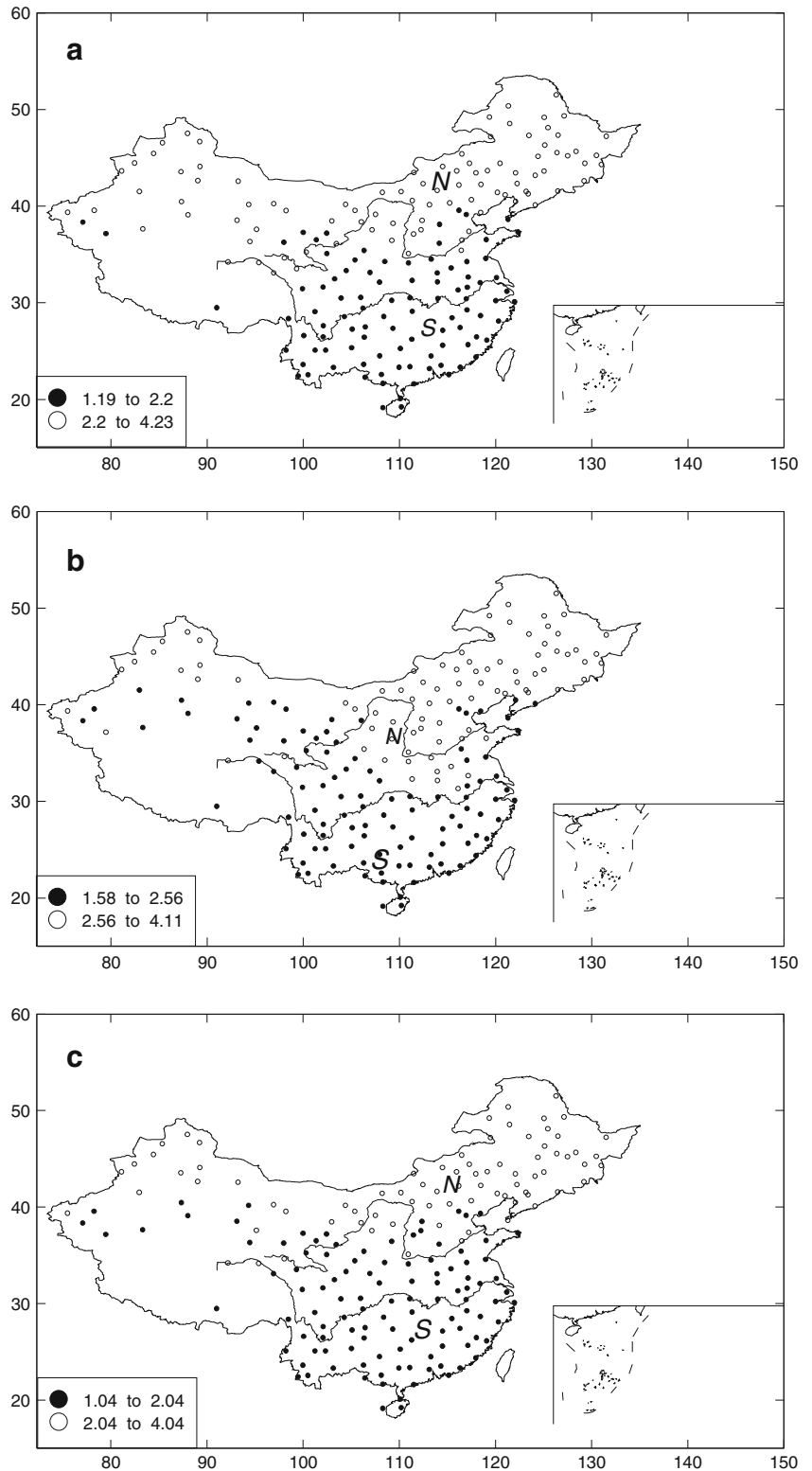
We can see clearly whatever the  $\chi$  values of the daily min, max, average temperature records, there are marked subarea characteristics when we choose  $\chi = \bar{\chi} - 1/5 \times \sigma_{\bar{\chi}}$ , with the critical  $\chi$  values are 2.20, 2.56, 2.04. There exists an obvious

change for such three time series, in which the whole China can be divided into two areas in Fig. 6. We find the  $\chi$  values in such two regions are consistent with dry/wet distributions in the south–north areas over China. The index  $\chi$  may provide a clue to climate forecast and evaluation.

### 6 Conclusions and discussions

The daily min, max, average temperature fluctuations are found to be long-range correlated and their average scaling exponent  $\alpha=0.69\pm 0.05$  indicates that there exists a stronger

**Fig. 6** The geographical distributions of the index  $\chi$ . **a** Minimum temperature records. **b** Maximum temperature records. **c** Mean temperature records



persistence for the daily min, max, average temperature fluctuations over China than that of the temperature fluctuations of earlier claims (Bunde et al. 1998; Fraedrich and Blender 2003). Positive long-range correlations are detected from 3 months to 3 years for each weather station. Exponents values is increasing with increasing distance from latitude in continent (as shown in Fig. 3, areas 1–4) and such distributions are not visible on the figure given by Fraedrich and Blender (2003) and Kiraly and Janosi (2005). Furthermore, scaling exponents of the daily temperature fluctuations are variable from station to station. In other words, the scaling exponent is not universal for continental stations over China.

Scaling exponent values are decreasing with the increasing distance from east shore only within smaller distances, which seems not to be affected by sea–land difference. The scaling exponent values in area SW, especially Yunnan province, are higher than these in adjacent regions, this may be caused by sea–land difference, southwest monsoon, and big landform factors' interactions. There exists the high scaling index values in area NW and NE, which may be due to the exchanges of south and north weather systems, Tibet Plateau landform, Siberian high pressure and monsoon and so on.

The  $\chi$  values of the min, max, average temperature records exhibit marked subarea characteristics when we choose  $\chi = \bar{\chi} - 1/5 * \sigma_{\bar{\chi}}$ . There exists an obvious change for such three time series, in which the whole China can be divided into two areas. We find the  $\chi$  values in such two regions are consistent with dry/wet distributions in the south–north areas over China.

**Acknowledgment** Many thanks are due to supports from National Natural Science Foundation of China (no. 40775040) and from Program of the Chinese Academy of Sciences (KLOCAW1106).

## References

- Bunde A, Havlin S (2002) Power-law persistence in the atmosphere and in the oceans. *Physica A* 314:15
- Bunde KE et al (1996) Analysis of daily temperature fluctuations. *Physica A* 231:393
- Bunde KE et al (1998) Indication of a universal persistence law governing atmospheric variability. *Phys Rev Lett* 81
- Bunde A et al (2000) Correlated and uncorrelated regions in heart-rate fluctuations during sleep. *Phys Rev Lett* 85:3736
- Bunde A et al (2001) Long term persistence in the atmosphere: global laws and tests of climate models. *Physica A* 302:255
- Bunde A et al (2004) Return intervals of rare events in records with long-term persistence. *Physica A* 342:308
- Bunde KE et al (2006) Long-term persistence and multifractality of river runoff records: detrended fluctuation studies. *J Hydrol* 322:120
- Cayan DR et al (2001) Changes in the onset of spring in the western United States. *Bull Am Meteorol Soc* 82(3):399
- Chen Z et al (2002) Effect of nonstationarities on detrended fluctuation analysis. *Phys Rev E* 65:041107
- Chen X, Lin G, Zuntao Fu (2007) Long-range correlations in daily relative humidity fluctuations: a new index to characterize the climate regions over China. *Geophys Res Lett* 34:L07804
- Dai AG, Trenberth KE, Karl TR (1998) Global variations in droughts and wet spells: 1900–1995. *Geophys Res Lett* 25:3367
- Eichner JF et al (2003) Power-law persistence and trends in the atmosphere—a detailed study of long temperature records. *Phys Rev E* 68:046133
- Fraedrich K, Blender R (2003) Scaling of atmosphere and ocean temperature correlations in observations and climate models. *Phys Rev Lett* 90:108510
- Govindan RB et al (2001) *Physica A* 294:239
- Govindan RB et al (2002) Global climate models violate scaling of the observed atmospheric variability. *Phys Rev Lett*. doi:10.1103/PhysRevLett.89.028501, Vol. 89; Issue 2
- Govindan RB et al (2003) *Physica A* 318:529
- Hansen JE, Sato M, Ruedy R et al (1998) *Science* 281(5379):930
- Heneghan C, McDarby G (2000) *Phys Rev E* 62:6103
- Hsu HH, Liu X (2006) *Geophys Res Lett* 30:2066
- Hu K et al (2001) Effect of trends on detrended fluctuation analysis. *Phys Rev E* 64:011114
- Jones PD (1988) *J Clim* 1(6):654
- Kantelhardt JW et al (2001) Detecting long-range correlations with detrended fluctuation analysis. *Physica A* 295:441
- Kiraly A, Janosi IM (2005) Detrended fluctuation analysis of daily temperature records: geographic dependence over Australia. *Meteorol Atmos Phys* 88:119
- Kurnaz ML (2004a) Application of detrended fluctuation analysis to monthly average of the maximum daily temperatures to resolve different climates. *Fractals* 12(4):365
- Kurnaz ML (2004b) Detrended fluctuation analysis as a statistical tool to monitor the climate. *J Stat Mech Theor Exp* P07009
- Lennartz S, Bunde A (2009) Trend evaluation in records with long-term memory: application to global warming. *Geophys Res Lett* 36:L16706
- Ma Z, Fu C (2003) *Glob Planet Chang* 37:189
- Manabe S, Wetherald RT (1987) *J Atmos Sci* 44:1211
- Manabe S, Wetherald RT, Stouffer RJ (1981) *Climate Chang* 3(4):336
- Monetti RA et al (2003) Long term persistence in the sea-surface temperature fluctuations. *Physica A* 320:581
- Peng C-K et al (1994) Mosaic organization of DNA nucleotides. *Phys Rev E* 49:1685
- Peng C-K et al (1995) *Chaos* 5:82
- Pielke RA et al (2002) *Int J Climatol* 22:421
- Robert T et al (2001) Cambridge University Press, 1–46
- Rybski D, Bunde A (2009) On the detection of trends in long-term correlated records. *Physica A* 388:1687
- Rybski D, Bunde A, von Storch H (2008) Long-term memory in 1000 years simulated temperature records. *J Geophys Res-Atmos* 113(D2):D02106
- Talkner P, Weber RO (2000) Power spectrum and detrended fluctuation analysis: application to daily temperatures. *Phys Rev E* 62(1):150
- Vyushin D, Zhidkov Z, Havlin S, Bunde A, Brenner S (2004) Volcanic forcing improves atmosphere-ocean coupled general circulation model scaling performance. *Geophys Res Lett* 31: L10206
- Weber RO, Talkner P (2001) Spectra and correlations of climate data from days to decades. *J Geophys Res-Atmos* 106(D17):20131
- Wetherald RT, Manabe S (1999) *Clim Chang* 43:495
- Wetherald RT, Manabe S (2002) *J Geophys Res* 107:4379
- WMO and UNEP (1990) New York: Cambridge University Press
- Wu GX, Zhang YS (1998) *Mon Weather Rev* 126:913
- Zhai PM, Pan XH (2003) *Geophys Res Lett* 30:1913
- Zhai PM, Zhang XB, Wan H, Pan XH (2004) Trends in total precipitation and frequency of daily precipitation extremes over China. *J Clim* 18:1096
- Zou XK, Zhai PM, Zhang Q (2005) Variations in droughts over China, 1951–2003. *Geophys Res Lett* 32:L04707
- Zwiers FW (2002) *Nature* 416:690